Solar-Terrestrial Physics. 2023. Vol. 9. Iss. 3. P. 68–76. DOI: 10.12737/stp-93202308. © 2023 N.A. Kurazhkovskaya, A.Yu. Kurazhkovskii. Published by INFRA-M Academic Publishing House

UDC 550.385.4
DOI: 10.12737/stp-93202308

Received May 04, 2023
Accepted July 06, 2023

HYSTERESIS EFFECT BETWEEN GEOMAGNETIC ACTIVITY INDICES (A_p, *Dst*) AND INTERPLANETARY MEDIUM PARAMETERS IN SOLAR ACTIVITY CYCLES 21–24

N.A. Kurazhkovskaya
Borok Geophysical Observatory, the Branch of Schmidt Institute of Physics of the Earth, RAS, Borok, Russia, knady@borok.yar.ru

A.Yu. Kurazhkovskii
Borok Geophysical Observatory, the Branch of Schmidt Institute of Physics of the Earth, RAS Borok, Russia, ksasha@borok.yar.ru

Abstract. We have studied the relationship of geomagnetic activity indices (A_p, *Dst*) on time intervals, equal to solar cycles (~11 years), with solar activity indicators and heliospheric parameters. It is shown that the plots of the A_p and *Dst* indices versus solar activity indicators, as well as versus heliospheric parameters, i.e. solar wind and IMF parameters in the ascending and descending phases of solar activity cycles 21–24 do not coincide, which is indicative of the hysteresis phenomenon. The A_p and *Dst* indices form hysteresis loops with all parameters we analyze during cycles 21–24. The shape and area of the hysteresis loops, as well as the direction of rotation, clockwise or counterclockwise, depend significantly on indicators of solar activity, heliospheric parameters and change from cycle to cycle. We have found a tendency for the extension and area of the hysteresis loops to decrease from cycle 21 to cycle 24. Analysis of the variability in the shape and size of the hysteresis loops formed by the A_p and *Dst* indices with solar indicators and heliospheric parameters gives reason to believe that the obtained loops reflect the long-term evolution of the solar wind energy flux, which determines global geomagnetic activity and the magnetospheric ring current intensity in the ascending and descending phases of solar activity cycles 21–24.

Keywords: geomagnetic activity, solar wind, solar activity cycles, heliospheric parameters, hysteresis.

INTRODUCTION

In many studies such as [Donnelly, 1991; Bachmann, White, 1994; Özgüç et al., 2012; Bruevich et al., 2018], it has been observed that the dynamics of a number of solar activity parameters is different during ascending and descending phases of solar cycle. In other words, the trajectory of changes in one solar activity parameter depending on the other demonstrates a similarity to hysteresis during a solar cycle. Research papers most often examine in pairs the relationships between such solar activity indicators as sunspot number, solar radio flux at a wavelength of 10.7 cm, solar flare index, maximum velocity of coronal mass ejections, etc. As an example, we refer to the papers [Bachmann, White, 1994; Özgüç et al., 2000, 2012; Bruevich et al., 2018] in which the effect of hysteresis between sunspot number and other solar activity indicators has been found. As is argued by Bachmann and White [1994], hysteresis is a real phenomenon, and not the result of instrumental effects and estimates of time shifts between solar activity indices and sunspot number.

The hysteresis is characteristic not only of solar indicators, but also of heliospheric parameters, ionospheric activity indices, as well as cosmic ray intensity. For instance, the effect of hysteresis between ionospheric and solar activity indices has been studied in [Kane, 1992; Ortiz de Adler, Elias, 2008; Bruevich et al., 2016; Deminov et al., 2020]. The hysteresis between cosmic ray intensity and sunspot number, as well as the solar flare index has been analyzed in [Mavromichalaki et al., 1998; Kane, 2003; Özgüç, Ataç, 2003; Singha et al., 2008] and many others. Recent decadal studies [Dmitriev et al., 2002; Özgüç et al., 2016; Reda et al., 2023] have revealed a hysteresis cycle of solar wind (SW) and interplanetary magnetic field (IMF) parameters: SW density *N*, velocity *V*, dynamic pressure P_{dyn}, IMF intensity *B* with Wolf numbers and other solar activity indicators.

Various indices are used to measure geomagnetic activity. The most commonly used indices are A_p and *Dst*, which measure global magnetic disturbance and magnetospheric ring current intensity during geomagnetic storms. Correlations of A_p and *Dst* indices with solar activity, SW and IMF parameters have been studied in many works, for example [Ahluwalia, 2000; Papitashvili et al., 2000; Verbanac et al., 2011; Kilcik et al., 2017; Samsonov et al., 2019]. These and other works provide correlation coefficients between the geomagnetic indices and heliospheric parameters, and estimate time shifts between different parameters. At the same time, the number of publications on the hysteresis effect between the geomagnetic indices and the solar activity indicators is very limited. We can mention the work [Özgüç et al., 2016], in which the hysteresis effect of A_p and *Dst* with the CME maximum velocity index was found only in cycle 23 and during the ascending phase of cycle 24. Bruevich et al. [2016] briefly mention a hysteresis between A_p and the solar radio flux at a wavelength of 10.7 cm in solar cycle 21. According to the

literature available to us, the question of whether the relationship between geomagnetic activity and solar activity indicators in other solar cycles is of hysteresis nature remains open. Moreover, it is interesting to find out whether the A_p and *Dst* indices form hysteresis loops with the IMF parameters in the last four solar cycles, for which the most complete satellite observations are available.

This paper is an attempt to identify the phenomenon of hysteresis of geomagnetic indices (A_p and *Dst*) with solar indicators, SW and IMF parameters in solar cycles 21–24, as well as to examine features of the hysteresis effect in different solar cycles.

1. DATA

As initial data we have used 27-day averages of Wolf numbers *W*, solar radio flux at a wavelength of 10.7 cm *F*10.7, geomagnetic indices A_p and *Dst*, SW and IMF parameters for the period from 1976 to 2019 from the OMNI database [https://spdf.gsfc.nasa.gov/pub/data/omni/low_res_omni/]. We deal with the following key SW and IMF parameters, as well as their combinations: velocity *V*, proton density *N*, IMF intensity *B*, IMF B_z component, proton temperature *T*, dynamic pressure P_{dyn}, and SW parameter β, in the definitions given to them on the OMNI website [https://omniweb.gsfc.nasa.gov/html/ow_data.html/], SW electric field E_y component: $E_y=-VB_z$, the ratio between helium ion and proton densities N_α/N_p. In addition, we have used annual averages of these parameters from the OMNI database.

The interval of interest covers four solar cycles — from 21 to 24. Information about the time of beginning, maximum, and minimum of the solar activity cycles was taken from [Ishkov, 2013]. We have analyzed the paired relationships of A_p and *Dst* with solar indicators and heliospheric parameters during the time periods equal to solar cycles.

2. RESULTS

2.1. Cyclic variation in solar activity, heliospheric parameters, and geomagnetic activity

When analyzing long-term variations in solar and geomagnetic activity indices, as well as in SW and IMF plasma parameters, their annual averages are usually used. Before examining the relationship of the geomagnetic activity indices with solar activity and heliospheric parameters in a separate solar cycle, let us take a look at the variation in their annual averages during the last four solar cycles.

Figure 1, *a*, *b* illustrates the dynamics of annual averages of the analyzed solar activity indices, interplanetary medium, and geomagnetic indices in solar cycles 21–24. The qualitative behavior of cyclic variations in the SW and IMF parameters is generally the same in cycles 21–24, although the cycles differ in duration and maximum amplitude. For instance, the variation in the solar radio flux *F*10.7 is similar to the cyclic variation in the sunspot number. The *F*10.7 value strictly follows the solar cycle in all its phases.

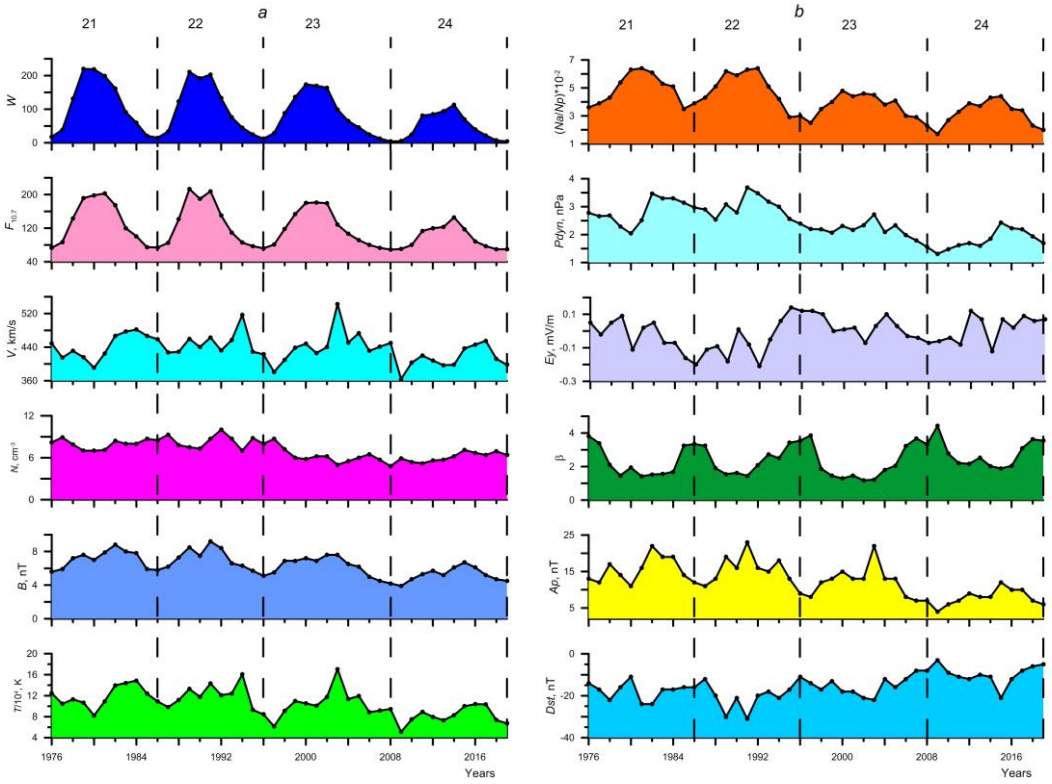

Figure 1. Dynamics of annual average solar activity indices, interplanetary medium parameters, and geomagnetic indices in solar cycles 21–24 (from top to bottom): Wolf numbers *W*, solar radio flux at a wavelength of 10.7 cm *F*10.7, SW velocity *V*, density *N*, IMF modulus |*B*|, temperature *T* (*a*); helium ion-to-proton density ratio N_α/N_p, SW dynamic pressure P_{dyn}, SW electric field E_y, SW parameter β, A_p and *Dst* geomagnetic activity indices (*b*)

The annual SW velocity V is maximum during the descending phase of solar activity when the probability of observing high-speed streams from coronal holes on the Sun is the highest [Holappa et al., 2014]. The ascending phase of all solar cycles features minimum annual average V. A similar cyclic variation is characteristic of the proton temperature T. Unlike the dynamics of V and T, the dynamics of the proton density N has two small maxima in the ascending and descending phases of solar activity. Minimum N is observed at solar maximum and minimum.

Long-term variations in the IMF intensity B (see Figure 1, *a*) and the helium ion-to-proton density ratio N_α/N_p (see Figure 1, *b*) change in phase with solar cycles. During each solar cycle, B and N_α/N_p are seen to increase and decrease during the ascending and descending phases of solar activity respectively. Maximum and minimum B and N_α/N_p coincide with the years of solar maxima and minima. The lowest annual averages of P_{dyn} and V are observed in the ascending phase of solar cycles. At solar maximum, P_{dyn} reaches the highest values. The descending phase of solar activity displays a tendency for P_{dyn} to decrease. Variations in the averaged SW electric field E_y component differ significantly during the same phases of the solar cycles. For example, in the descending phase of cycle 21, E_y decreases, whereas in the descending phase of cycle 22, on the contrary, it increases. Figure 1 does not illustrate the behavior of the IMF B_z component since it is mirrored by the variation in the E_y component. Long-term variations in the β parameter are in antiphase to solar cycles: β reaches the highest and lowest values in the years of solar minimum and maximum respectively.

The geomagnetic indices A_p and *Dst* measure the level of geomagnetic disturbance, which significantly depends on solar activity and interplanetary medium conditions. In the long-term evolution of A_p, the 11-year periodicity of solar activity is clear-cut (see Figure 1, *b*). The cyclic variation in A_p has two maxima: one near solar maximum, the other in the descending phase of solar activity, as has been previously observed in [Schreiber, 1998]. The variation in annual average *Dst* mirrors the annual average behavior of A_p. The annual average variations in *Dst* coincide with the variation in the plasma parameter β, as has been previously noted in [Kurazhkovskaya et al., 2021], and the long-term variations in A_p are in antiphase to the β parameter variation in all solar cycles (see Figure 1, *b*).

Thus, during solar cycles 21–24, different heliospheric parameters change in phase, antiphase, or with some time shift relative to solar activity. In other words, the variation in each heliospheric parameter depends significantly on solar cycle phase. Note that the typical behavior of the annual average SW and IMF parameters during cycles 21–24 coincides with the previously observed patterns of behavior of heliospheric parameters in Earth's orbit for previous solar cycles [Veselovsky et al., 1998; Dmitriev et al., 2009].

2.2. Hysteresis effect of geomagnetic and solar activity

Let us analyze the relationship of the geomagnetic indices A_p and *Dst* with solar activity indicators during solar cycles 21–24. We take Wolf numbers W and the solar radio flux at a wavelength of 10.7 cm $F10.7$ as solar activity indicators. The time series of 27-day averages of both A_p, *Dst* and solar indicators in each cycle contain short-period fluctuations, which we smoothed using the running average method. Figure 2 shows in pairs the relationships of A_p and *Dst* with W and $F10.7$ in the last four solar cycles. The relationships were obtained from 27-day averages of the parameters previously smoothed by a running average over 27 points. Variations in $A_p(W)$, $Dst(W)$, $A_p(F10.7)$, and $Dst(F10.7)$ for different solar cycles are marked with circles: cycle 21 with blue, cycle 22 with red, cycle 23 with light blue, cycle 24 with pink circles.

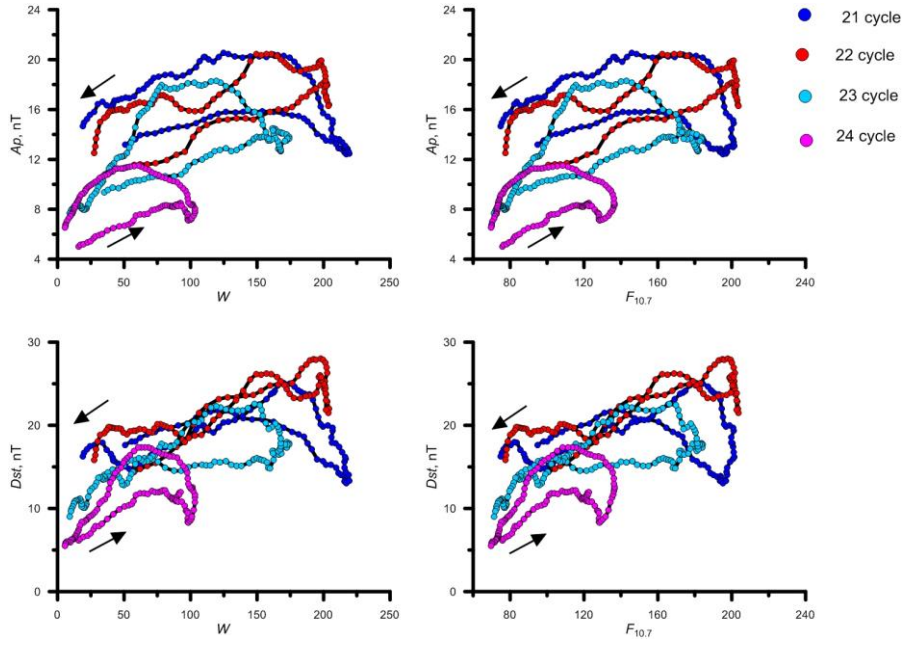

Figure 2. Hysteresis loops between geomagnetic activity indices A_p and *Dst* (|*Dst*|) and solar activity indicators W and $F10.7$ for solar cycles 21–24

Figure 2 indicates that two different values of A_p or *Dst* correspond to the same fixed *W* or *F*10.7. As a result, in each solar cycle the relationships of A_p and *Dst* with *W* and *F*10.7 do not coincide during ascending and descending phases of solar activity. This behavior of $A_p(W)$, *Dst*(*W*), $A_p(F\ 10.7)$, and *Dst*(*F*10.7) in the solar activity cycles resembles the hysteresis phenomenon. Referring to Figure 2, the curves of geomagnetic indices versus solar activity indicators have a shape close to hysteresis loops, with $A_p(W)$, *Dst*(*W*), $A_p(F10.7)$, and *Dst*(*F*10.7) forming hysteresis loops in each solar cycle.

The qualitative characteristics of hysteresis loops are their shape, width (the distance between the ascending and descending phases), and area. Comparative analysis of hysteresis loops has revealed their similarity and difference in different solar cycles. For example, the hysteresis loops formed by the A_p index with *W* and *F10*.7 are similar in shape and size in all solar cycles. Such similarity is typical of *Dst*(*W*) and *Dst*(*F*10.7). This pattern is likely to be due to the identical cyclic behavior of *W* and *F*10.7 (see Figure 1, *a*). As for sizes of the hysteresis loops formed by A_p and *Dst*, the loops for $A_p(W)$ and $A_p(F10.7)$ are wider than those for *Dst*(*W*) and *Dst*(*F*10.7).

Figure 2 clearly demonstrates the evolution of hysteresis from one solar cycle to another. For example, one of the features of $A_p(W)$, $A_p(F10.7)$, *Dst*(*W*), and *Dst*(*F*10.7) is a gradual decrease in the extension and area of hysteresis loops from cycle 21 to cycle 24. Furthermore, as shown in Figure 2, the loops shift along the horizontal axis to the zero point of the vertical axis from cycle 21 to cycle 24. We think that such dynamics and variation in size of hysteresis loops reflect a decrease in solar and geomagnetic activity over time. The hysteresis loops of $A_p(W)$, $A_p(F10.7)$, *Dst*(*W*), and *Dst*(*F*10.7) have the smallest area in solar cycle 24, which is characterized by a significant decrease in the amplitude of solar indicators and geomagnetic activity indices as compared to other cycles.

As is known, a necessary condition for the occurrence of hysteresis loops is a phase shift between the parameters we analyze. The width of hysteresis loops is proportional to the phase shift (time delay) between geomagnetic indices and solar activity indicators and actually reflects the time delay between the magnetospheric response and the processes occurring on the Sun. Referring to Figure 2, the width of hysteresis loops may be comparable in different solar cycles, but may also differ significantly. The longer the time delay, the wider the loop. The time delay between pairs of geomagnetic activity indices and solar indices is not constant in a particular cycle and may decrease or increase. Visual comparison between hysteresis loops shows that the widest loops were observed during cycle 23 in the dependences of both A_p and *Dst* on *W* and *F*10.7. The most pronounced hysteresis effect in the dependences of A_p and *Dst* on *W* and *F*10.7 is manifested in the last two solar cycles. In cycles 21 and 22, the hysteresis loops of *Dst*(*W*) and *Dst*(*F*10.7) have a more complex structure than those of $A_p(W)$ and $A_p(F10.7)$.

Another characteristic of hysteresis loops is the direction of rotation, which reflects the delay between one parameter and the other.

Arrows in Figure 2 indicate the direction of rotation in hysteresis cycles. For instance, in the hysteresis loops formed by A_p with *W* and *F*10.7, changes occur counterclockwise in all the solar cycles considered, which indicates a delay in the change of global geomagnetic disturbance (which is measured by A_p) relative to the change of solar indicators. Moreover, with the same fixed *W* or *F*10.7, the A_p index in the ascending is significantly lower than that in the descending phase. This pattern is valid for all the cycles we analyze.

In the hysteresis loops formed by *Dst* with *W* and *F*10.7, the direction of rotation is also counterclockwise in all the solar cycles. Thus, manifestations of magnetospheric disturbance associated with the development of geomagnetic storms lag behind a change in solar indicators. The resulting curves (see Figure 2) indicate a non-linear relationship of A_p and *Dst* with *W* and *F*10.7.

2.3. Hysteresis cycle of geomagnetic activity and SW and IMF parameters

Next we examined the relationship of the geomagnetic activity indices with interplanetary medium parameters in solar cycles 21–24. To do this, the relationships of A_p and *Dst* with SW and IMF plasma parameters were considered in pairs. We found that the relationships of A_p and *Dst* with the heliospheric parameters form hysteresis loops with all the parameters under study. Here, we do not give all the relationships obtained, but limit ourselves to presenting the relationships of A_p and *Dst* with only some basic parameters such as *B*, *V*, *T*, N_α/N_p, as well as with P_{dyn} and β, which are a combination of the key SW and IMF parameters.

Figure 3 shows in pairs the relationships of A_p and *Dst* with the SW and IMF parameters: *B* and *V* (*a*); *T* and N_α/N_p (*b*); P_{dyn} and β (*c*) in solar cycles 21–24. As in Section 2.2, all the relationships were obtained from 27-day averages, pre-smoothed by a running average over 27 points. The general pattern in this case is that the trajectories of variations in A_p and *Dst* depending on interplanetary parameters do not coincide in the ascending and descending phases of the solar cycles. This allows such a feature to be considered as the hysteresis phenomenon.

As follows from the plots obtained, the hysteresis effect of A_p and *Dst* with the IMF intensity, the helium ion-to-proton density ratio, and the β parameter is regular. Hysteresis loops of a more complex configuration are formed by A_p and *Dst* with SW velocity, temperature, and dynamic pressure. By the complex structure of hysteresis loops we mean the intersection of the ascending and descending branches of hysteresis, as, for example, in *Dst*(P_{dyn}) and $A_p(N_\alpha/N_p)$ during solar cycles 21 and 22 and in $A_p(N_\alpha/N_p)$ during cycle 23. Nevertheless, in the relationship of A_p and *Dst* with *V*, *T*, P_{dyn} there are indicators of hysteresis. The same complex hysteresis loops are formed by A_p and *Dst* with the SW density *N* and the electric field component E_y (not shown here).

Both the area and the shape of the hysteresis loops of A_p and *Dst* differ significantly depending on heliospheric parameters. So, $A_p(B)$, $A_p(T)$, $A_p(P_{dyn})$ represent

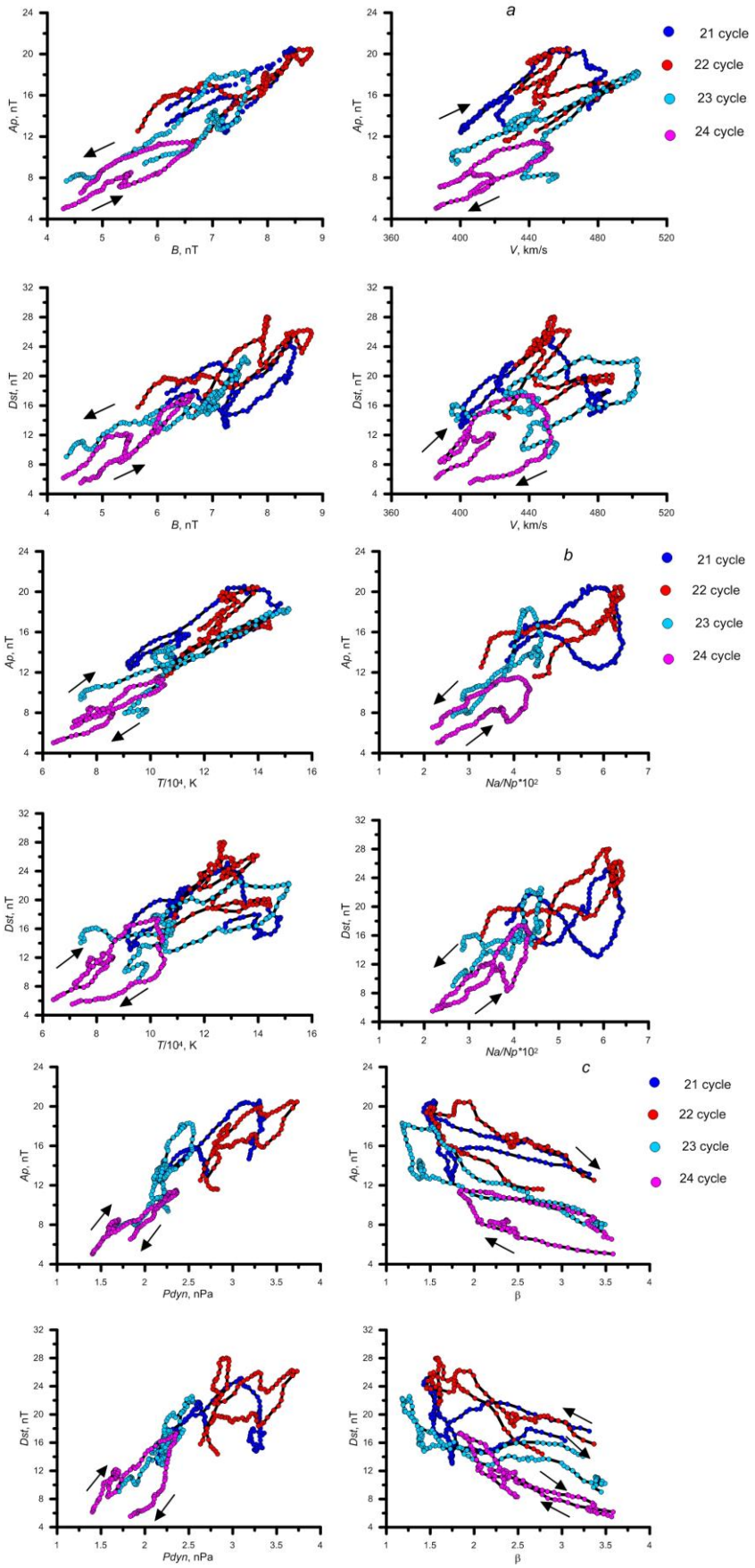

Figure 3. Hysteresis effect for the A_p and *Dst* indices (|*Dst*|) as function of IMF intensity *B* and SW velocity *V* (*a*); proton temperature *T* and helium ion-to-proton density ratio N_α/N_p (*b*); SW dynamic pressure P_{dyn} and β parameter (*c*) in solar cycles 21–24

narrower hysteresis loops than $A_p(V)$, $A_p(N_\alpha/N_p)$, $A_p(\beta)$. The *Dst* index forms relatively narrow hysteresis loops only with *B* and P_{dyn}; and with the rest of the parameters, wide loops. As noted above, the width of the hysteresis loops at a qualitative level reflects the time delays between the parameters in the ascending and descending phases of solar cycle. The wider the hysteresis loop, the longer the time delays. Accordingly, it can be said that the time delays between A_p and *B*, *T* and P_{dyn} are shorter than between A_p and N_α/N_p, β. The time delays between *Dst* and *B*, P_{dyn} are shorter than between other parameters. In other words, the delay in the magnetospheric response to changing external conditions is manifested in the size of hysteresis loops.

Besides, there is a relationship between the area of hysteresis loops and solar activity. Areas of the loops formed by A_p and *Dst* with all the heliospheric parameters gradually decrease from cycle 21 to cycle 24. One of the features of the hysteresis loops obtained for A_p and *Dst* is their displacement along the X-axis to the low point of the Y-axis from cycle 21 to cycle 24 with an increase in the heliospheric parameters. A similar tendency is observed for all the parameters except for the β parameter, the slope of the hysteresis loops of which is opposite to the slope of the hysteresis loops of other parameters. The fact of increasing geomagnetic activity with decreasing β has been observed in [Zotov et al., 2019; Kurazhkovskaya et al., 2021]. Since there is an inverse relationship between the geomagnetic activity indices and the β parameter, another slope of the hysteresis loops to the horizontal axis in $A_p(\beta)$ and *Dst*(β) becomes clear. All the hysteresis loops shown in Figure 3 point to a nonlinear relationship of A_p and *Dst* with the heliospheric parameters. The direction of rotation in the hysteresis loops formed by A_p and *Dst* differs depending on the parameters analyzed: for example, in the loops formed with the IMF intensity and the helium ion-to-proton density ratio, the direction of rotation is counterclockwise; and with the SW velocity, the proton temperature, the SW dynamic pressure, it is clockwise in all the cycles. With the counterclockwise direction of rotation at the same fixed value of *B* or N_α/N_p, A_p and *Dst* in the ascending phase of solar activity are lower than in the descending phase. In the case of clockwise rotation at a fixed value of, for example, *V*, *T*, P_{dyn}, A_p and *Dst* in the ascending phase are higher than in the descending phase. The counterclockwise direction of change in A_p and *Dst* depending on *B* and N_α/N_p can be interpreted as a delay in changes of geomagnetic activity relative to changes of these interplanetary parameters, similar to the delay in changes of geomagnetic activity relative to changes of solar indicators. The clockwise direction of rotation in the hysteresis loops means that A_p and *Dst* variations are ahead of *V*, *T*, P_{dyn} variations. All this shows that in a solar cycle, the interplanetary medium parameters due to the existing time shifts between them, make a different contribution to the global disturbance and the ring current intensity. The direction of rotation in the hysteresis loops formed by A_p and *Dst* with different heliospheric parameters generally coincides, except for the β parameter. In the loops formed by *Dst* with the β parameter, the direction of rotation is counterclockwise in odd cycles and clockwise in even cycles. In the hysteresis loops formed by A_p with the β parameter, changes occur clockwise in all the solar cycles we analyze.

3. DISCUSSION

The 11-year periodicity of solar activity is manifested both in the dynamics of SW and IMF parameters and in geomagnetic disturbance. Examining in pairs the relationship of the geomagnetic indices A_p and *Dst* with solar indices and heliospheric parameters, we have found that curves of A_p and *Dst* versus *W* and *F*10.7, as well as versus the SW and IMF parameters in the ascending and descending phases of solar cycles 21–24 do not coincide. The return of $A_p(W)$, $A_p(F10.7)$, *Dst*(*W*), and *Dst*(*F* 10.7) to solar minimum occurs along a trajectory different from the trajectory of their motion to solar maximum. A similar behavior is typical of the relationship of A_p and *Dst* with the interplanetary medium parameters. The observed ambiguous relationship of geomagnetic activity indices with solar activity indices and with the heliospheric parameters during the ascending and descending phases of the solar cycles resembles the hysteresis effect. The analysis has shown that the relationships of A_p and *Dst* with solar activity, SW and IMF parameters in solar cycles 21–24 have the form of hysteresis loop for all the parameters considered. The hysteresis between A_p, *Dst* and various parameters is a manifestation of their cyclic behavior (see Figure 1). As follows from Figures 2 and 3, hysteresis loops in different solar cycles differ in shape, width (the distance between the ascending and descending phases), area, and direction of rotation. Some loops have a complex structure, sometimes the ascending and descending branches of the hysteresis may intersect. At the same time, all the plots obtained show a decrease in the extension and area of the hysteresis loops from cycle 21 to cycle 24. The smallest area of the hysteresis loops formed by A_p and *Dst* with different parameters is characteristic of solar cycle 24.

In our opinion, the processes occurring on the Sun and in the interplanetary medium, as well as the change in the energy of the SW stream entering the magnetosphere as a result of the interaction of IMF with the geomagnetic field, manifest themselves as a decrease in the area of hysteresis loops from cycle 21 to cycle 24. As is known, one of the main causes of solar activity variability is a change in the topology and intensity of the solar magnetic field. According to [Penn, Livingston, 2010], since 1998 there has been a decrease in the intensity of the magnetic field of sunspots, which continued in solar cycles 23 and 24. The processes occurring inside the Sun in recent decades [McIntosh et al., 2019] lead to a decrease in the solar magnetic field [Janardhan et al., 2015]. The decrease in the solar magnetic field during cycles 23 and 24 is closely related to IMF weakening, a decrease in the SW parameters, changes in the interplanetary medium structure and in the regime of the SW flow around the magnetosphere [Yermolaev et al.,

2022]. Amplitudes of the last solar cycles have also noticeably decreased [Hathaway, 2015]. The low solar activity causes changes in the interaction between IMF and the geomagnetic field and in the intensity of SW energy flux into Earth's magnetosphere. The decrease in solar activity ultimately leads to a decrease in geomagnetic activity and manifests itself in a gradual decrease in the area of hysteresis loops from cycle 21 to cycle 24.

Based on the variability of the shape and size of the hysteresis loops formed by A_p and *Dst* with the parameters considered, it can be assumed that the loops reflect the long-term evolution of the SW energy flux, which determines global geomagnetic activity and ring current intensity during the ascending and descending phases of solar cycles 21–24.

It is generally believed that the hysteresis effect is a long-term feature of solar activity cycles. At the same time, hysteresis manifests itself not only in the time periods comparable to the duration of solar cycles, but also in shorter time periods. For example, Ptitsyna et al. [2021] have found the hysteresis effect in the cosmic ray cutoff rigidity when comparing it with the dynamics of geomagnetic indices and interplanetary medium parameters during a strong geomagnetic storm.

Let us consider another example of observing hysteresis in a relatively short time period. In [Kurazhkovskaya et al., 2021], attention was drawn to the nonlinear nature of the relationship between *Dst* and the β parameter during geomagnetic storms. Indeed, having previously smoothed the accumulated hourly data on the *Dst* index and the β parameter from [Kurazhkovskaya et al., 2021] by a running average, we plot *Dst*(β) for the interval of 168 hrs from storm commencements. This time interval covers the average duration of the storm main phase, which, according to [Yermolaev et al., 2007], is 7±4 hrs, and the storm recovery phase, which on average lasts for 5–7 days. Figure 4 displays the obtained dependences *Dst*(β) for 288 geomagnetic storms with sudden (*a*) and 645 storms with gradual commencement (*b*) observed from 1964 to 2010.

It can be seen that the trajectory of variation in the *Dst* index depending on the β parameter in the storm main phase is seen to differ from its trajectory in the recovery phase. This is a typical indicator for hysteresis. During geomagnetic storms, *Dst* and β vary cyclically. Specifically, *Dst*(β) has the form of a hysteresis loop for storms with both sudden and gradual commencements. Thus, the *Dst*(β) relationship clearly demonstrates the hysteresis effect during geomagnetic storms.

Hysteresis loops for storms with sudden and gradual commencements differ in width and direction of rotation. For example, in a hysteresis loop formed by the *Dst* index with the β parameter during storms with sudden commencement, changes occur clockwise and the loop formed is narrow (see Figure 4, *a*). During storms with gradual commencement, a hysteresis loop is significantly wider and the direction of rotation is counterclockwise (see Figure 4, *b*).

In this paper, we want to draw attention to the fact that the hysteresis of geomagnetic activity exists both in time periods equal to solar cycles and in shorter time periods. A more detailed study on the quantitative characteristics of hysteresis loops formed by geomagnetic activity indices with heliospheric parameters may be useful for predicting solar and geomagnetic activity, as well as for understanding the physical processes responsible for the solar and geomagnetic activity relationship

CONCLUSION

We have examined the relationship of geomagnetic activity indices (A_p, *Dst*) with solar activity indicators (*W*, *F*10.7) and heliospheric parameters in the last four solar cycles. We have found that the curves of A_p and *Dst* versus *W* and *F*10.7, as well as versus the SW and IMF parameters in the ascending and descending phases of solar cycles 21–24 do not coincide, which we interpret as an indicator of hysteresis. It is shown that the geomagnetic indices A_p and *Dst* form hysteresis loops with all the parameters considered. We have established that the shape, width, and area of the hysteresis loops, as well as the direction of rotation (clockwise or counterclockwise) significantly depend on SW parameters and vary from cycle to cycle. The area of hysteresis loops is shown to decreases from cycle 21 to cycle 24. The smallest area of the hysteresis loops formed by A_p and *Dst* with different parameters is characteristic of solar cycle 24, which is associated with a tendency for solar activity indicators, interplanetary medium parameters, and hence geomagnetic activity to decrease. The hysteresis cycles for A_p and *Dst* confirm the existence of time

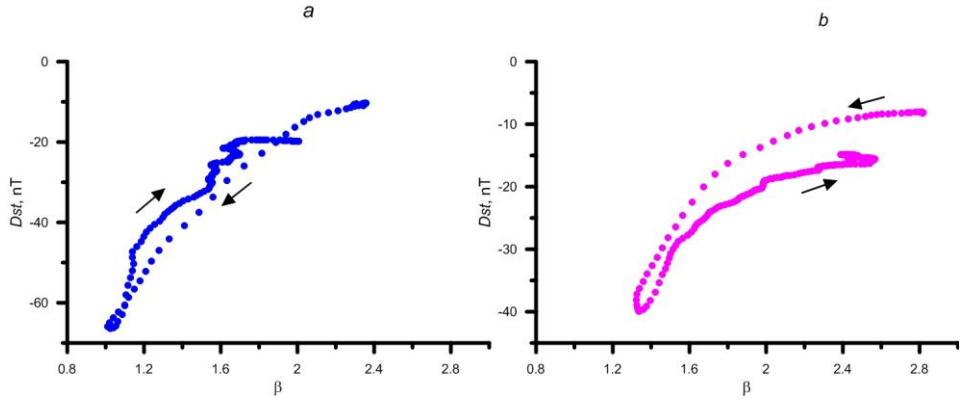

Figure 4. Hysteresis effect between the *Dst* index and the β parameter during geomagnetic storms with sudden (*a*) and gradual commencements (*b*)

delays between geomagnetic activity and processes on the Sun and in SW during the ascending and descending phases of the cycle. The hysteresis phenomenon points to a nonlinear relationship of A_p and *Dst* with solar activity and heliospheric parameters. The evolution of hysteresis loops from cycle 21 to cycle 24 reflects the difference in the SW energy flux that determines global geomagnetic activity and magnetospheric ring current intensity in the ascending and descending phases.

We thank the creators of the OMNI database (Goddard Space Flight Center, NASA, USA) for the opportunity to use 27-day averages and annual averages of Wolf numbers (*W*), solar radio flux at a wavelength of 10.7 cm (*F*10.7), geomagnetic indices (A_p and *Dst*), SW and IMF parameters. We express our sincere gratitude to B.I. Klain for his interest in the work and discussion of the results.

The work was carried out under Government assignment of Borok Geophysical Observatory of IPE RAS No. FMWU-2022-0027.

REFERENCES

Ahluwalia H.S. *Ap* time variations and interplanetary magnetic field intensity. *J. Geophys. Res*. 2000, vol. 105, no. A12, pp. 27,481–27,487. DOI: 10.1029/2000JA900124.

Bachmann K., White O.R. Observations of hysteresis in solar-cycle variations among seven solar-activity indicators. *Solar Physics*. 1994, vol. 150, pp. 347–357. DOI: 10.1007/BF00712896.

Bruevich E.A., Kazachevskaya T.V., Katyushina V.V., Nusinov A.A., Yakunina G.V. Hysteresis of indices of solar and ionospheric activity during 11-year cycles. *Geomagnetism and Aeronomy*. 2016, vol. 56, no. 8, pp. 1075–1081. DOI: 10.1134/S0 01679321608003X.

Bruevich E.A., Bruevich V.V., Yakunina G.V. Cyclic variations in the solar radiation fluxes at the beginning of the 21st century.*Moscow University Physics Bulletin*. 2018, vol. 73, no. 2, pp. 216–222. DOI: 10.3103/S0027134918020030.

Deminov M.G., Nepomnyashchaya E.V., Obridko V.N. Solar activity indices for ionospheric parameters in the 23rd and 24th cycles. *Geomagnetism and Aeronomy*. 2020, vol. 60, pp. 1–6. DOI: 10.1134/S0016793220010053.

Dmitriev A.V., Suvorova A.V., Veselovsky I.S. Expected hysteresis of the 23-rd solar cycle in the heliosphere. *Adv. Space Res.* 2002, vol. 29, iss. 3, pp. 475–479. DOI: 10.1016/S0273-1177(01)00615-9.

Dmitriev A.V., Suvorova A.V., Veselovsky I.S. Statistical Characteristics of the heliospheric plasma and magnetic field at the Earth's orbit during four solar cycles 20–23. *Handbook on Solar Wind: Effects, Dynamics and Interactions*. Chapter 2. New York, NOVA Science Publ., 2009, pp. 81–144.

Donnelly R.F. Solar UV spectral irradiance variations. *J. Geomagn. Geoelectr. Suppl*. 1991, vol. 43, pp. 835–842.

Hathaway D.H. The Solar Cycle. *Living Rev. Solar Phys*. 2015, vol. 12(4). DOI: 10.1007/lrsp-2015-4.

Holappa L., Mursula K., Asikainen T. A new method to estimate annual solar wind parameters and contributions of different solar wind structures to geomagnetic activity. *J. Geophys. Res: Space Phys*. 2014, vol. 119, pp. 9407–9418. DOI: 10.1002/2014JA020599.

Ishkov V.N. Reduced and extended periods of solar activity: Monitoring features and key facts. *Proc. National Yearly Conf.* "*Solar and Solar-Terretstrial Physics 2013"*. Saint Petersburg, 2013. P. 111–114 (In Russian).

Janardhan P., Bisoi S.K., Ananthakrishnan S., Tokumaru M., Fujiki K., Jose L., Sridharan R. A 20 year decline in solar photospheric magnetic fields: Inner-heliospheric signatures and possible implications. *J. Geophys. Res.: Space Phys*. 2015, vol. 120, pp. 5306–5317. DOI: 10.1002/2015JA021123.

Kane R.P. Solar cycle variation of *f*oF2. *J. Atmos. Terr. Phys*. 1992, vol. 54, no. 9, pp. 1201–1205.

Kane R.P. Lags, hysteresis, and double peaks between cosmic rays and solar activity. *J. Geophys. Res.* 2003, vol. 108, iss. A10, 1379. DOI: 10.1029/2003JA009995.

Kilcik A., Yiğit E., Yurchyshyn V., Ozguc A., Rozelot J.P. Solar and Geomagnetic Activity Relation for the Last two Solar Cycles. *Sun and Geosphere*. 2017, vol. 12/1, pp. 31–39.

Kurazhkovskaya N.A., Zotov O.D., Klain B.I. Relationship between geomagnetic storm development and the solar wind parameter β. *Solar-Terr. Phys.* 2021, vol. 7, iss. 4. pp. 24–32. DOI: 10.12737/stp-74202104.

McIntosh S.W., Leamon R.J., Egeland R., Dikpati M., Fan Y., Rempel M. What the sudden death of solar cycles can tell us about the nature of the solar interior. *Solar Phys*. 2019, vol. 294, no. 88. DOI: 10.1007/s11207-019-1474-y.

Mavromichalaki H., Belehaki A., Rafios X. Simulated effects at neutron monitor energies: evidence for a 22-year cosmic-ray variation. *Astron. Astrophys.* 1998, vol. 330, pp. 764–772.

Ortiz de Adler N., Elias A.G. Latitudinal variation of f_oF2 hysteresis of solar cycles 20, 21 and 22 and its application to the analysis of long-term trends. *Ann. Geophys*. 2008, vol. 26, pp. 1269–1273. DOI: 10.5194/angeo-26-1269-2008.

Özgüç A., Ataç T. Effects of hysteresis in solar cycle variations between flare index and cosmic rays. *New Astronomy*. 2003, vol. 8, iss. 8, pp. 745–750. DOI: 10.1016/S1384-1076(03)00063-0.

Özgüç A., Ataç T., Antalova A. Effects of hysteresis of some solar indices during the past three solar cycles 20, 21 and 22. *Proc. 1st Solar and Space Weather Euroconference "The Solar Cycle and Terrestrial Climate"*. Santa Cruz de Tenerife, Spain, 2000. SP–463. pp. 403–405.

Özgüç A., Kilcik A., Rozelot J.P. Effects of hysteresis between maximum CME speed index and typical solar activity indicators during cycle 23. *Solar Phys*. 2012, vol. 281, pp. 839–846. DOI: 10.1007/s11207-012-0087-5.

Özgüç A., Kilcik A., Georgieva K., Kirov B. Temporal Offsets between maximum CME speed index and solar, geomagnetic, and interplanetary indicators during solar cycle 23 and the ascending phase of cycle 24. *Solar Phys.* 2016, vol. 291, pp. 1533–1546. DOI: 10.1007/s11207-016-0909-y.

Papitashvili V.O., Papitashvili N.E., King J.H. Solar cycle effects in planetary geomagnetic activity: Analysis of 36-year long OMNI dataset. *Geophys. Res. Lett*. 2000, vol. 27, no. 17, pp. 2797–2800.

Penn M.J., Livingston W. Long-term evolution of sunspot magnetic fields. *Proc. IAU Symp. "The Physics of Sun and Star Spots"*. 2010, vol. 273, pp. 126–133.

Ptitsyna N.G., Danilova O.A., Tyasto M.I. Phenomena of hysteresis in the cutoff rigidity of cosmic rays during the superstorm of November 7–8, 2004. *Geomagnetism and Aeronomy*. 2021, vol. 61, pp. 483–491. DOI: 10.1134/S0016793221040137.

Reda R., Giovannelli L., Alberti T. On the time lag between solar wind dynamic parameters and solar activity UV proxies. *Adv. Space Res*. 2023, vol. 71, iss. 4, pp. 2038–2047. DOI: 10.1016/j.asr.2022.10.011.

Samsonov A., Bogdanova Y.V., Branduardi-Raymont G., Safrankova J., Nemecek Z., Park J.-S. Long-term variations in solar wind parameters, magnetopause location, and geomagnetic activity over the last five solar cycles. *J. Geophys. Res.: Space Phys*. 2019, vol. 124, pp. 4049–4063. DOI: 10.1029/2018JA026355.

Schreiber H. On the periodic variations of geomagnetic activity indices A_p and *ap*. *Ann. Geophys*. 1998, vol. 16, pp. 510–517.

Singha M., Singha Y.P., Badruddin. Solar modulation of galactic cosmic rays during the last five solar cycles. *Journal of Atmospheric and Solar-Terrestrial Physics*. 2008, vol. 70, pp. 169–183.

Verbanac G., Vršnak B., Veronig A., Temmer M. Equatorial coronal holes, solar wind high-speed streams, and their geoeffectiveness. *Astronomy Astrophys*. 2011, vol. 526, no. A20. DOI: 10.1051/0004-6361/201014617.

Veselovsky I.S., Dmitriev A.V., Suvorova A.V. Average parameters of the solar wind and interplanetary magnetic field at the Earth's orbit for the last three cycles. *Solar System Research*. 1998, vol. 32, no. 4, pp. 310–315.

Yermolaev Y.I., Yermolaev M.Y., Lodkina I.G., Nikolaeva N.S. Statistical investigation of heliospheric conditions resulting in magnetic storms. *Cosmic Research*. 2007, vol. 45, no. 1, pp. 1–8. DOI: 10.1134/S0010952507010017.

Yermolaev Y.I., Lodkina I.G., Khokhlachev A.A., Yermolaev M.Y. Peculiarities of the heliospheric state and the solar-wind/magnetosphere coupling in the era of weakened solar activity. *Universe*. 2022, vol. 8, 495. DOI: 10.3390/universe8100495.

Zotov O.D., Klain B.I., Kurazhkovskaya N.A. Influence of the β solar wind parameter on statistical characteristics of the A_p index in the solar activity cycle. *Solar-Terr. Phys.* 2019, vol. 5, no. 4, pp. 46–52. DOI: 10.12737/stp-54201906.

URL: https://spdf.gsfc.nasa.gov/pub/data/omni/low_res_omni/ (accessed December 8, 2022).

URL: https://omniweb.gsfc.nasa.gov/html/ow_data.html/ (accessed December 8, 2022).

Original Russian version: Kurazhkovskaya N.A., Kurazhkovskii A.Yu., published in Solnechno-zemnaya fizika. 2023. Vol. 9. Iss. 3. P. 73–82. DOI: 10.12737/szf-93202308. © 2023 INFRA-M Academic Publishing House (Nauchno-Izdatelskii Tsentr INFRA-M)

How to cite this article

Kurazhkovskaya N.A., Kurazhkovskii A.Yu. Hysteresis effect between geomagnetic activity indices (A_p, *Dst*) and interplanetary medium parameters in solar activity cycles 21–24. *Solar-Terrestrial Physics*. 2023. Vol. 9. Iss. 3. P. 68–76. DOI: 10.12737/stp-93202308.